



6th International Conference On Advances In Computing & Communications, ICACC 2016, 6-8
September 2016, Cochin, India

A Design of Digital Microfluidic Biochip along with Structural and Behavioural Features in Triangular Electrode based Array

Piyali Datta^{a,*}, Amartya Dutta^b, Riya Majumder^b, Arpan Chakraborty^b, Debasis Dhal^b,
Rajat Kumar Pal^b

^a Department of Computer Science and Engineering, Heritage Institute of Technology, Chowbaga Road, Anadapur, Kolkata 700 107, West Bengal, India

^b Department of Computer Science and Engineering, University of Calcutta, JD-2, Sector – III, Saltlake, Kolkata – 700 106, West Bengal, India

Abstract

Digital microfluidic based biochip manoeuvres on the theory of microfluidic technology, having a broad variety of applications in chemistry, biology, environmental monitoring, military etc. Being concerned about the technological advancement in this domain, we have focused on equilateral triangular electrodes based DMFB systems. Accepting the associated design issues, here, we have addressed many facets of such electrodes regarding their structural and behavioural issues in comparison to the existing square electrodes. As the requisite voltage reduction is a key challenging design issues, to implement all the tasks using triangular electrodes that are possible in square electrode arrays as well, is a tedious job. Furthermore, to deal with this new design deploying triangular electrodes, we have analyzed all the necessary decisive factors including fluidic constraints to ensure safe droplet movements and other modular operations together with mixing and routing. Moreover, an algorithm has been developed to find a route for a given source and destination pair in this newly designed DMFB. Finally, we have included a comparative study between this new design and the existing one while encountering the above mentioned issues.

© 2016 The Authors. Published by Elsevier B.V. This is an open access article under the CC BY-NC-ND license (<http://creativecommons.org/licenses/by-nc-nd/4.0/>).

Peer-review under responsibility of the Organizing Committee of ICACC 2016

Keywords: Digital microfluidics; Triangular Electrode; PCB layer Mixing; Routing; Assay

* Corresponding author. Tel.: +91-964-779-1193.
E-mail address: piyalidatta150888@gmail.com

1. Introduction

Digital Micro-Fluidic Biochips possess the ability to execute a wide-range of biochemical laboratory protocols on a 2D array of electrodes, and hence, addressed as a ‘*lab-on-a-chip*’¹. DMFB controls nano-liter or micro-liter volume of biological samples and reagents under the EWOD principle^{2,3}. The modular operations that are executed on a DMFB in order to accomplish an assay as a whole are dispensing of droplets, routing of sample and reagent droplets towards allied modules for mixing, and then the detection of some intended parameter(s) in the mixed droplet^{2,3,4}. Though in the existing works we are mostly accustomed with square shaped electrodes to embrace a droplet, electrode plates with other shapes are also possible^{5,6}. For an example, regular hexagonal electrodes have the capability to hold a droplet as well as to incorporate proper movement of the droplet⁵. Another such design is possible through electrodes that are equilateral triangular in shape⁶. As triangular electrodes are concerned, in this paper, we have discussed how the fundamental operations, i.e., mixing, routing etc. and other design issues may lead to a betterment with this geometrical change. In this regard, we have also mentioned various factors associated with this design like the size⁶, fluidic constraints⁶, pin constraints, and wiring of the electrodes to carry on all the modular operations safely on the newly proposed triangular electrode based biochip or simply *TEDMB*.

Nomenclature

y	the side of a <i>TEDMB</i> electrode
a	the side of a square electrode

2. Preliminaries

2.1. Relative Study comprising both Square and Equilateral Triangular Electrodes

To avoid contamination⁷ during routing, a safe distance between any two droplets has to be maintained raising the requirement of some constraints. There are two types of fluidic constraints², static fluidic constraints and dynamic fluidic constraints.

- *Static Fluidic Constraints in traditional DMFB*^{2,3}:

If there are two droplets D_i and D_j at time t , on a square electrode array, avoidance of inadvertent mixing can be performed maintaining at least one electrode gap between them, i.e., $|X_i(t) - X_j(t)| \geq 2$ and $|Y_i(t) - Y_j(t)| \geq 2$.

While moving to the next cell, they shift to new positions at time instant $(t+1)$. Thus, at time $(t+1)$, the gap between the new locations must also be at least two, i.e., $|X_i(t+1) - X_j(t+1)| \geq 2$ and $|Y_i(t+1) - Y_j(t+1)| \geq 2$.

- *Dynamic Fluidic Constraints in traditional DMFB*^{2,3}:

$|X_i(t+1) - X_j(t)| \geq 2$ and $|Y_i(t+1) - Y_j(t)| \geq 2$, i.e., the new location of D_i cannot be adjacent to the location (unchanged) of D_j .

In this context, *TEDMB* also offers a number of fluidic constraints to perform the operations without fluidic hazards⁴.

- *Horizontal Static and Dynamic Fluidic Constraints in TEDMB*⁶:

This is same as that of traditional DMFB, i.e., $|X_i(t) - X_j(t)| \geq 2$ and $|X_i(t+1) - X_j(t+1)| \geq 2$ for static fluidic constraints whereas $|X_i(t+1) - X_j(t)| \geq 2$ and $|X_i(t) - X_j(t+1)| \geq 2$ are the dynamic fluidic constraints.

- *Vertical Static and Dynamic Fluidic Constraints TEDMB*⁶:

In a *TEDMB* array the triangular electrodes may be classified into two types. If the movement of droplet to the upward direction is restricted, the electrode is classified as *Type 1* electrode. On the flip side, restriction of the movement to the downward direction, categorize the *Type 2* electrodes; as shown in Fig. 1(a). Considering this assumptions, the vertical fluidic constraint is: $|Y_i(t) - Y_j(t)| \geq 2$ and $|Y_i(t+1) - Y_j(t+1)| \geq 2$. $|Y_i(t) - Y_j(t+1)| \geq 2$ and $|Y_i(t+1) - Y_j(t)| \geq 2$, i.e., the new location of D_i cannot be adjacent to the old location of D_j .

2.2. Size of the Electrodes

In [6] authors proposed *TEDMB* design keeping the portion of the droplet outside a square electrode is same for

the *TEDMB* electrode to ensure requisite overlapping to the directly neighbours to guarantee a sufficient surface tension gradient for movement. A comprehensive calculation: $y = 1.73a = \sqrt{3}a$, where ‘ y ’ is the side of a *TEDMB* electrode and ‘ a ’ is the side of a square electrode make us to conclude that $y > a$. Moreover, the junction of four square electrodes (2×2 array) forms a square of side $a/2$. Thus, the length of the principal diagonal of a square formed by four adjacent square electrodes becomes $a/2\sqrt{2}$, whereas the junction of six equilateral triangular electrodes forms a regular hexagon of side $a/2$ (see Fig. 1(b)), and hence, the length of the principal diagonal = $\{2 \times (\text{length of a side of the regular hexagon})\} = 2 \times (a/2) = a^4$.

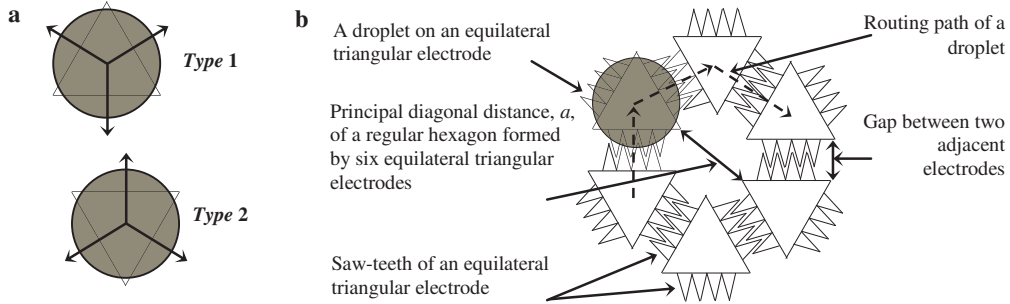


Fig. 1. (a) Two types of electrode with droplet movement directions; (b) Top view of a droplet on an equilateral triangular electrode. Here saw-teeth of adjacent electrodes are arranged closer but not short circuited.

2.3. Pin Constrained Chip Design in DMFB

As the movement of a droplet is only possible by controlling its surface tension gradient², control pins are used to apply the external voltage. An efficient design should consume less voltage that introduces pin count reduction to be a problem of utmost importance⁸. Several pin designs have been proposed among whom array based partitioning⁹, broadcasting¹⁰, electrode cross referencing¹¹ are popular. The minimum number of pins required for a single droplet movement throughout all the electrodes on a 2D array, without droplet interference², is denoted by k , which is the number of independent control pins necessary. It could also be visualized as a graph colouring problem, where the value of k is 5^{12} (see Fig. 2(a)). Thus, in general the value of k is never less than 5. Using *Connect-5* algorithm^{3,9} a PCB (Printed Circuit Board) of three layers could be devised, where each layer may contain at most two non-overlapping wire layout connecting the sets of two pins individually³, differentiated by numbers (see Fig. 2(b)).

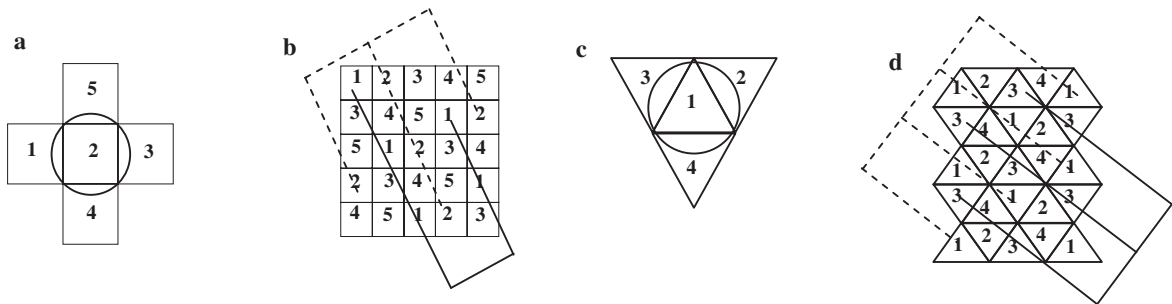


Fig. 2. (a) Pin number 2 is a droplet holder that has four direct neighbour pins 1, 3, 4, and 5; (b) A 5×5 array is covered by five pins using *Connect-5* structure and its wire representation for pins 1 and 2 only (in a layer); (c) A *TEDMB* cell holding droplet at position 1 and its three direct neighbours of positions 2, 3, 4; (d) A *TEDMB* array partition using four control pins.

3. Contribution

The main contribution of this paper is a new model of a DMF biochip system with equilateral triangular electrode array having privileges over processing time of assay operations like mixing and routing. Moreover, other design issues have been considered with their associated complexities as well as the improvements while we shift our focus to the newly proposed triangular electrode based biochip or simply *TEDMB*. Now, the main contributions in this paper are as follows.

- A pin constrained design for *TEDMB* that requires lesser number of control pins to drive individual electrodes satisfying all the fluidic constraints than that of the earlier square electrodes array³. Thus the design becomes efficient for low power consumption as a whole.
- A quantitative study of processing elements, i.e., mixers or diluters, has been done between traditional DMFB with square electrodes and newly designed *TEDMB* with equilateral triangular electrodes. We can conclude that the diffusion in an ongoing mixing (or dilution) process is evidently better in terms of percentage calculation of mixing, in *TEDMB*.
- A routing algorithm is presented here that finds a route between any pair of *TEDMB* cells. The algorithm has been evaluated experimentally as well. As the routing between 92.1% of the source-destination pairs among the chip demand same number of unit movements with respect to traditional DMFB, a better mixing in *TEDMB* ensures enhancement in assay completion time as a whole.

3.1. Pin Constrained Chip Design in *TEDMB*:

- *Design issues*

Each electrode is essentially activated and deactivated ensuring safe movement of a droplet. Now for a *TEDMB* array having N^2 electrodes, controlling each of them requires N^2 pins in a brute force method that gives rise to required cost of $O(N^2)$. To reduce the effective cost pin count must be within a reasonable amount such that the design suits well in a practical scenario and this lead to develop a design where a control pin is shared among a group of electrodes^{2,9,10,11}. In this context, sharing of control pins may result in droplet interference that is caused by the inadvertent activation of electrodes at any time instant. Our proposed *CTNT-4* algorithm identifies that only four pins are sufficient to hold a droplet ‘safely’ and thereby requiring only four control pins to construct a partition.

- *Minimum Number of Pins Satisfying Electrode Constraints:*

In a 2D microfluidic array, the problem of finding a minimum number of independent control pins requisite to have a full control of a single droplet without interference, can be reduced to the well-known graph colouring problem. The problem of finding chromatic number of a graph is an NP-complete problem¹². Moreover, pins at those three neighbours must be mutually different in order to maintain safe movement of a droplet. In general the dual of a 2D *TEDMB* array is a regular graph with degree three, hence cannot be coloured by less than four pins. Fig. 2(c) shows the layout of a *TEDMB* sub-array assigning the electrodes by four distinct control pins.

- *Pin Assignment Algorithm:*

We have already come across the pin assignment problem for a single electrode associated with its direct neighbours. Now, our objective is to extend this assignment for a chip of size $m \times n$ as a whole. *CTNT-4* algorithm in Fig. 2(c) performs this with the concept to *Connect Three Neighbouring Triangles by 4* pins. In *CTNT-4*, starting from the first row of a partition, pins are assigned in a cyclic order until the boundary is reached (line 4 through line 14). In the next row, the same order is maintained but two cells (in pin number) are shifted to the left or right (we choose to shift right here; line 16). This process is continued until all cells in the partition are assigned pin numbers (line 3 through line 17).

- *Wiring Solution and Printed Circuit Board:*

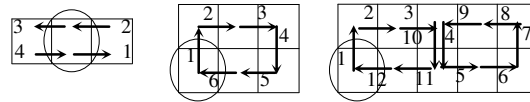
A layout of a partition assigned with control pins using *CTNT-4* has been depicted in Fig. 3(a). A wiring solution essentially connects the electrodes having same pin with electrical wires lying on a printed circuit board (PCB). An

efficient wiring solution should solve the problem with lesser number of PCB layers. Here, in *TEDMB*, we connect all the electrodes by two-layer PCB, instead of three as in the case of traditional DMFB^{2,3}, avoiding electrical hazards due to crossing. Fig. 2(d) shows the wire connection in a PCB layer connecting pins ‘1’ and ‘3’ in isolation.

a CTNT-4 (R, C, i, j)

1. Set $(i, j) =$ Top Left Electrode of the Partition
2. $N = 1$
3. **While** $i \leq R$ **do**
4. **While** $j \leq C$ **do**
5. **If** $N \leq 4$ **then**
6. Assign $i, j \rightarrow N$
7. $N = N + 1$
8. **End If**
9. **Else**
10. $N = 1$
11. Assign $i, j \rightarrow N$
12. $N = N + 1$
13. $j = j + 1$
14. **End While**
15. $i = i + 1$
16. $N = N + 2$
17. **End While**

b



Droplet
flow path \rightarrow

c

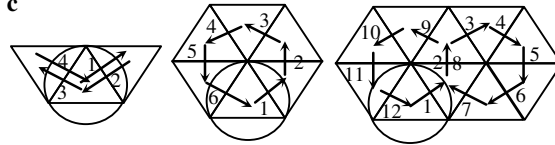


Fig. 3. (a) Algorithm *CTNT-4* for pin assignment in *TEDMB* array; (b) Movement of a droplet in 1×3 mixer (oscillation), 2×3 mixer (circular) and a 2×5 mixer (zigzag) of square electrodes; (c) Movement of a droplet in 1×3 mixer (oscillation), 2×3 mixer (circular) and a 2×5 mixer (zigzag) of triangular electrodes.

3.2. *TEDMB* Processing Elements:

The mixing process dominates any operation performed in a biochip over time as it needs a huge number of iteration (say 1000 cycles) towards its completion¹³. The cells for a possible assignment of a mixer are chosen from a dedicated mixer library as a form of a $p \times q$ sub-array. Now, we have two stuffs at hand: either we have to find a ‘good’ scheduling algorithm taking the mixer type as rectangular/non-rectangular or perform some modifications in the technology behind that can possibly find a better mixer that takes less amount of time to accomplish given operation⁴.

Fig. 3(b) shows the processing elements of a DMF biochip with square electrodes. The authors of [14] have compared intelligently the mixing operation in terms of phase changes during consecutive movements through a mixing module. We will redefine the thought and design various mixers in *TEDMB* that certainly reduce completion time of a given assay operation. Depending on the phase changes three types of movements are familiar in general, namely, forward movement (M_f) for phase change of 0° , orthogonal movement (M_o) due to phase change of 90° , and backward movement (M_b) while the phase change is of 180° . Taking the cell to cell droplet velocity as 20 cm/s^3 , we can calculate the percentage of mixing in a given type of mixer. As the active mixing is proportional to the rate of diffusion^{2,3} we can formally state the followings: $M_b < M_o < M_f$ in terms of contribution towards the completion of mixing. From this conclusion, we draw the relation between the rate of diffusion (D) and the phase change (ϕ) of movement, i.e., $D \propto \frac{1}{\phi}$ that eventually explains that a ‘good’ mixer should avoid M_b as well as M_o by introducing 60° phase change (M_a) throughout a mixing cycle, leading an enhancement to the diffusion rate (D) and the percentage mixing as well¹⁴. As a mixing process consists of typically more than 1000 such mixing cycles¹³, the fractional improvement in each cycle contributes reasonably in overall mixing time.

3.3. TEDMB Routing:

To maintain the timing constraints^{2,3}, an efficient droplet routing in a microfluidic array has to be developed that fundamentally finds a low cost path between any two cells or any two modules and thus, it is an utmost important design issue. Fig. 4 shows *TZ_Routing* algorithm in *TEDMB* array for finding out a minimal cost route between any source-destination pair. It outputs the number of unit movement requisite for moving a droplet between a source-destination pair (\mathcal{S} , \mathcal{D}) that is provided as an input to the algorithm. Considering the relative position of the destination with the source, \mathcal{D} may be on the same row, same column, on the diagonal to \mathcal{S} , or any other position. The algorithm starts from this decision making process. If both \mathcal{S} and \mathcal{D} belong to the same row, only row movement is performed to reach the destination (line 5) while routing of the droplet is to be done through a column if they share same column. Due to the assumption of different types of triangular electrodes (type1 and type2) in the array, column movements are not identical for all types of \mathcal{S} , \mathcal{D} pairs.

For an example, in case of type1 electrode⁶, as the upward movement is restricted, the upward column movement starts by shifting one electrode row-wise that is essentially a type2 electrode⁶. Starting from type1 electrode at (i, j) , if it moves to the type2 cell at $(i, j + 1)$, it is shifted to $(i + 1, j + 1)$. Now, this is eventually a type1 electrode and then the droplet moves to $(i + 1, j)$, where the effective column movement is one from (i, j) . Thus, a droplet upward movement from a type1 electrode is not identical with a droplet downward movement. Hence, the requisite time depends on the type of the \mathcal{S} , \mathcal{D} pair as well as the direction of the movement. Table 1 shows the variations of required number of unit movement in different cases where n denotes the difference between the source and destination row values.

TZ_Routing(\mathcal{S} , \mathcal{D})

1. Set Source \mathcal{S} at (m, n)
2. Set Destination \mathcal{D} at (p, q)
3. $\mathcal{C} = 0$
4. **If** $m = p$ **then**
5. Perform_RowMove(\mathcal{S} , \mathcal{D})
6. $\mathcal{C} = \mathcal{C} + \text{Time_RowMove}(\mathcal{S}, \mathcal{D})$
7. **End If**
8. **Else If** $n = q$ **then**
9. Perform_ColumnMove(\mathcal{S} , \mathcal{D})
10. $\mathcal{C} = \mathcal{C} + \text{Time_ColumnMove}(\mathcal{S}, \mathcal{D})$
11. **End If**
12. **Else**
13. Perform_Z_Routing(\mathcal{S} , \mathcal{D})
14. $\mathcal{C} = \mathcal{C} + \text{Time_Z_Routing}(\mathcal{S}, \mathcal{D})$
15. **Return** \mathcal{C}

Fig. 4. Algorithm *TZ_Routing* to discover route between any two cells

Table 1. The number of unit movements between a cell pair

Source type	Destination type	Direction	Number of unit movement
T1 (T2)	T1 (T2)	Up (Down)	$2 \times n$
T1 (T2)	T2 (T1)	Up (Down)	$2 \times n + 1$
T2 (T1)	T1 (T2)	Up (Down)	$2 \times n - 1$
T2 (T1)	T2 (T1)	Up (Down)	$2 \times n$

Table 2. The positions of different diagonal cells with respect to a type-1 and type-2 electrode

	Type-1	Type-2
B_R_D	$(i+1, j), (i+1, j+1), (i+2, j+1), (i+2, j+2), (i+3, j+2), \dots$	$(i, j+1), (i+1, j+1), (i+1, j+2), (i+2, j+2), (i+2, j+3), \dots$
U_L_D	$(i, j-1), (i-1, j-1), (i-1, j-2), (i-2, j-2), (i-2, j-3), \dots$	$(i-1, j), (i-1, j-1), (i-2, j-1), (i-2, j-2), (i-3, j-2), \dots$
B_L_D	$(i+1, j), (i+1, j-1), (i+2, j-1), (i+2, j-2), (i+3, j-2), \dots$	$(i, j-1), (i+1, j-1), (i+1, j-2), (i+2, j-2), (i+2, j-3), \dots$
U_R_D	$(i, j+1), (i-1, j+1), (i-1, j+2), (i-2, j+2), (i-2, j+3), \dots$	$(i, j+1), (i-1, j+1), (i-1, j+2), (i-2, j+2), (i-2, j+3), \dots$

In the algorithm *TZ_Routing*, we perform *Z_Routing* (line 13) that finds a path from source to destination while the row or column numbers are different. Algorithm *Z_Routing* has been shown in Fig. 5(a). Now, we categorize the the cells other than the row electrodes and column electrodes, into two specific types: diagonal electrodes and zonal electrodes. To define a diagonal electrode with respect to a given source, we depict the cases in Table 2. However, rest of the cells are zonal electrodes, leading to a subdivision of eight zones depending on their relative positions as shown in Fig. 5(b). As an illustration, if an electrode is in zone one (i.e., Z_1) with coordinate (x,y) , *Z_Routing* computes the path along the diagonal from the source to (x, k) and then from (x, k) to (x, y) , where k denotes the column number that results from intersection between the diagonal and the destination row. Thus, to reach any destination cell other than a row or a column electrode with respect to a given source, *Z_Routing* moves the droplet through the diagonal up to the row (column) of the destination electrode as it takes minimum number of unit movements, and then the droplet traverse along that row (column) until the destination is reached. Line 8 to 13 of

Z_Routing, perform this by always measuring the time taken by diagonal and row moves (i.e., Δ_1) or diagonal and column moves (i.e., Δ_2) separately and taking the minimum of those.

```

a   Z_Routing(m, n, p, q)
1.   If (p, q) ∈ Zone_1 ∨ Zone_4 ∨ Zone_5 ∨ Zone_8 then
2.     Perform_DiagonalMove(m, n), (p, q)
3.     Perform_RowMove(p, q), (p, q)
4.      $\mathcal{C} = \mathcal{C} + \text{Time\_DiagonalMove}((m, n), (p, q)) +$ 
       Time_RowMove(p, q), (p, q)
5.   End If
6.   If (p, q) ∈ Zone_2 ∨ Zone_3 ∨ Zone_6 ∨ Zone_7 then
7.     Perform_DiagonalMove(m, n), (q, q)
8.      $\Delta_1 = \text{Time\_DiagonalMove}((m, n), (p, q)) +$ 
       Time_RowMove(p, q), (p, q)
9.      $\Delta_2 = \text{Time\_DiagonalMove}((m, n), (q, q)) +$ 
       Time_ColumnMove(q, q), (p, q)
10.    If  $\Delta_1 < \Delta_2$  then
11.      Perform_DiagonalMove(m, n), (p, q)
12.      Perform_RowMove(p, q), (p, q)
13.       $\mathcal{C} = \mathcal{C} + \Delta_1$ 
14.    End If
15.    Else
16.      Perform_DiagonalMove(m, n), (q, q)
17.      Perform_ColumnMove(q, q), (p, q)
18.       $\mathcal{C} = \mathcal{C} + \Delta_2$ 
19.    End If
20.  Return  $\mathcal{C}$ 
    
```

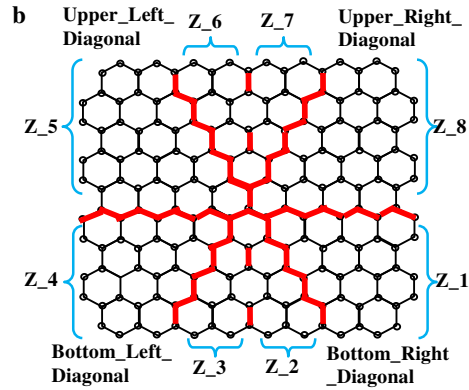


Fig. 5. (a) Algorithm *Z_Routing* to find route from source to a cell which shares neither same column nor same row with the source; (b) Subdivision of zones in a *TEDMB* array.

4. Experimental Results

Table 3. Comparison table for DMFB and *TEDMB*

Features	Traditional DMFB	<i>TEDMB</i>
Droplet radius	R	R
Side of an electrode	A	$\sqrt{3}a$
Gap between two electrodes	$a/2$	$a/2$
Portion of a droplet outside electrode	$0.207a$	$0.207a$
Junction of the four electrodes	a square with diagonal $a/\sqrt{2}$	hexagon with principle diagonal a
Droplet movement	Along four directions	Along three directions
Minimum pin requirement	5	4
# PCB layers	3; thus, high hazardous (electrically)	2; thus, electrically less hazardous
Mixer zone	Square or rectangle	Hexagon

Here, we point out some of the major structural and behavioural features of *TEDMB* and compare it to traditional DMFB in Table 3. Moreover, in traditional DMFB only Manhattan path is followed for a route, whereas for *TEDMB* in *TZ_Routing*, the routing path does not necessarily pursue a Manhattan path. An experimental study implying these is shown in Table 4 and Fig 6. It is evident that the route cost for *TZ_Routing* for most of the source destination pairs is either same or less than that of the square electrode. At this moment we can straightforwardly proclaim that if $T(A)$ denotes the assay completion time in the associated design, then the followings hold true:

$$T(A_{\text{TEDMB}}) = T(\text{Routing}_{\text{TEDMB}}) + T(\text{Mixing}_{\text{TEDMB}}) \quad T(A_{\text{DMFB}}) = T(\text{Routing}_{\text{DMFB}}) + T(\text{Mixing}_{\text{DMFB}})$$

As mixing dominates the routing with respect to time, and *TEDMB* offers an enhanced mixing operation using a series of phase changes (stating $T(\text{Mixing}_{\text{TEDMB}}) \leq T(\text{Mixing}_{\text{DMFB}})$), placing consecutive modules at suitable positions

(that have the lower route cost in *TEDMB*) we may achieve lower assay completion time on an average, i.e., $T(A_{TEDMB}) \leq T(A_{DMFB})$.

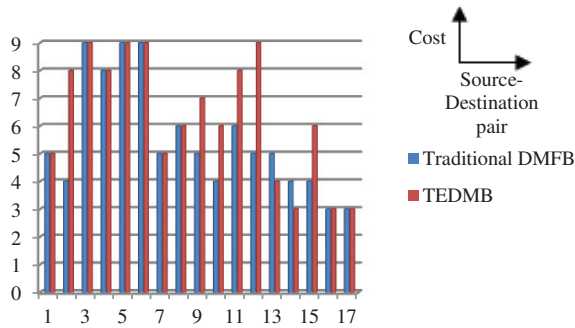


Fig. 6. Route performance of DMFB and *TEDMB*

Table 4. Route Cost Comparison between DMFB and *TEDMB*

Source (5, 5) and Destination (--, --)	Zone	Time for Square DMFB	Time for <i>TEDMB</i>
(5, 10)	Row	5	5
(1, 5)	Column	4	8
(9, 10)	Diagonal	9	9
(1, 1)	Diagonal	8	8
(1, 10)	Diagonal	9	9
(10, 1)	Diagonal	9	9
(4, 9)	Z ₋₈	5	5
(7, 9)	Z ₋₁	6	6
(8, 7)	Z ₋₂	5	7
(9, 3)	Z ₋₃	6	8
(7, 2)	Z ₋₄	5	4
(4, 2)	Z ₋₅	4	3
(2, 4)	Z ₋₆	4	6
(3, 4)	Z ₋₆	3	3
(3, 6)	Z ₋₇	3	3

5. Conclusions

While dealing with a microfluidic array of square electrodes^{2,3}, we observe that transformation of geometry of a chip modifies the route path of droplets that in turn possess an impact on the rate of diffusion between two droplets at the time of mixing, which is inversely proportional to the phase shift¹⁴. Thus, a better mixing due to an enhanced rate of diffusion per phase shift^{13,14}, fabrication of a chip with less number of layers in PCB², and a low cost route through the chip may be achieved through this design. However, every design, as a matter of fact, has its own turnover and limitations. As a route cost is lower than of DMFB and clearly, the percentage of mixing is comparatively better in *TEDMB*, it is the responsibility of ‘good’ scheduling algorithms that utilize only the routing region that has lower cost and thereby reducing the assay completion time on an average. Our probable future work will be to perform a route based online compilation in a *TEDMB* array, digging up improved assay completion time.

Reference

1. Fair R.B. Is a True Lab-on-a-Chip Possible? *Microfluid Nanofluid*; 2007; vol. 3, pp. 245-281.
2. Chakrabarty K. Design Automation and Test Solutions for Digital Microfluidic Biochips, *IEEE Transactions on Circuits and Systems*; 2010; vol. 57, no. 1, pp. 4-17.
3. Chang H.-C., Yeo L. *Electrokinetically Driven Microfluidics and Nanofluidics*, New York, NY: Cambridge University Press; 2009.
4. Ho T S. Design Automation for Digital Microfluidic Biochips, *International Conference on Solid-State and Integrated Circuit Technology (ICSICT)*; 2012; pp. 1-4.
5. Su F, Chakrabarty K, and Pamula V K. Yield Enhancement of Digital Microfluidics-Based Biochips Using Space Redundancy and Local Reconfiguration, *Proceedings of the Design, Automation and Test in Europe Conference and Exhibition (DATE)*; 2005.
6. Datta P, Dutta A, Majumder R, Chakraborty A, Dhal D, Pal R K. A Technology Shift towards Triangular Electrodes from Square Electrodes in Design of Digital Microfluidic Biochip, *IEEE ICECE*; 2014; pp. 1-4.
7. Lin C Y, Chang Y W. Cross-contamination Aware Design Methodology for Pin Constrained Digital Microfluidic Biochips, *IEEE Transactions on Computer-Aided Design of Integrated Circuits and Systems*; 2011; vol. 30, pp. 817–828.
8. Chakrabarty K and Xu T. *Digital Microfluidic Biochips, Design Automation and Optimization*. USA: CRC Press; 2010.
9. Xu T, Chakrabarty K. Droplet-trace-based array partitioning and a pin assignment algorithm for the automated design of digital microfluidic biochips, *IEEE/ACM ICH/SCSS*; 2006; pp. 112-117.
10. Zhao Y, Xu T, and Chakrabarty K. Broadcast electrode-addressing and scheduling methods for pin-constrained digital microfluidic biochips, *IEEE Transactions on Computer-Aided Design of Integrated Circuits and Systems*; 2011; vol. 30, Issue 7, pp. 986–999.
11. Yeung H C and Young F Y. General purpose cross-referencing Microfluidic Biochip with reduced pin-count, *Asia and South Pacific Design Automation Conference*; 2014; pp. 238–243.
12. Cormen T H, Leiserson C E, Rivest R L, et al. *Introductions to Algorithms*. 3rd ed. PHI learning Pvt. Ltd.; 2011.
13. Paik P, Pamula V K, Fair R B. Rapid Droplet Mixers for Digital Microfluidic Systems. *Lab-on-a-Chip*; 2003; pp. 253–259.
14. Alistar M, Pop P. Online Synthesis for Operation Execution Time; *International Symposium on Integrated Circuits (ISIC)*, IEEE; 2014; pp. 356-359.